The 2025 World Congress on
Advances in Structural Engineering and Mechanics (ASEM25)
BEXCO, Busan, Korea, August 11-14, 2025

Behavioral characteristics and ovality of shield TBM tunnel segment lining considering break - joint mode

Dong-Gun Lee[1], Hong-Joo Lee[2] *Ki-Il Song[3] and Gyeong-Ju Yi[4]
[1), 2) 3)]*Department of Civil Engineering, Inha University, Incheon 22212, Korea*
[4)] *SQ engineering, Seoul 05818, Korea*

[3)] ksong@inha.ac.kr

ABSTRACT

This study analyzes the behavior characteristics of segmental linings by applying the Break-Joint Mode (BJM, Gharehdash and Barzegar, 2015), an analytical method that considers segmentation, as an interpretation method for segmental lining. The analysis results using this model show that the segments and rings cause relative displacements in discrete block units. The BJM relatively well simulates the deformation patterns of segmental linings constructed in soil grounds, particularly in soft ground. The study reviewed the stresses acting on segmental linings under static loads. The analysis results showed that under static loading, the stress values obtained from the BJM were lower across all sections of the segmental lining compared to those from the NJM. After the tunneling process is completed, shield TBM tunnel segmental linings exhibit ovality. Although each country has its own ovality quality standard in the range of 5‰ to 10‰, these standards are not based on structural analysis results. The existing standards are difficult to achieve for shield TBM tunnels installed in soil grounds. The Break-Joint Mode applied in this study presents a method to redefine ovality quality standards based on structural analysis.

1. INTRODUCTION

Segmental linings used in shield TBM tunnels are composed of discrete segments and rings, structurally integrated through bolts and shear keys. Unlike continuous linings used in NATM tunnels, this segmented system inherently exhibits discontinuous mechanical behavior. In practice, however, there are reported cases where, after tunnel construction, bolts at the segment joints excluding the launch shaft area are deliberately loosened or removed to allow the segments to settle naturally into the surrounding ground (Ministry of Land, Transport and Maritime Affairs, 2011). This management

---

[1)] Research Fellow
[2)] PhD Student
[3)] Professor
[4)] Vice President

approach leads to relative displacement between segments, joint offsets, and opening gaps. Such geometric irregularities are particularly pronounced in soft ground conditions and often result in noticeable ovalization of tunnel cross-sections. Although many countries impose ovality quality standards within the range of 5‰ to 10‰, these criteria are largely empirical and lack structural analysis-based justification. Field observations of ovalities exceeding 50‰ highlight the need for a more rational, mechanics-based interpretation.

Conventional analytical approaches typically idealize segmental linings as continuous structures. The Non-Joint Mode (NJM) assumes full rigidity between segments and neglects joint behavior entirely, while two-ring beam–spring models attempt to simulate joint interactions through rotational and shear springs. However, these approaches are limited to two-dimensional representations. Furthermore, they fail to reflect the segment-level deformation characteristics such as inter-segmental displacements, localized stress concentrations, and segment-to-ring misalignments. As a result, current modeling approaches often diverge from the actual deformation patterns observed in the field.

To overcome these limitations, this study applies the Break-Joint Mode (BJM), which models the segmental lining using a friction-based interface without considering the structural contribution of bolts or shear keys. Coulomb-type interface elements are introduced at the joints to represent contact behavior between segments, enabling the simulation of discontinuous displacements and joint offsets. The objective of this study is to evaluate the static response characteristics of shield TBM segmental linings using the BJM, and to compare them against the results derived from NJM. Through this comparison, the study aims to identify critical differences in mechanical response, validate the field applicability of BJM, and ultimately propose a framework for structurally grounded ovality criteria, replacing the current empirical standards.

2. OVERVIEW OF SEGMENT LINING ANALYIS MODELS

2.1 Existing analysis methods and limitations

Structural analysis of segmental linings in shield TBM tunnels can be broadly categorized into analytical and numerical approaches. However, with the advancement of computational techniques, analytical methods have become largely obsolete. Numerical analyses are generally divided into continuum models and beam-spring models. In the continuum model, the ground is represented by elastoplastic elements, and the segmental lining is assumed to be a continuous structure. In contrast, the beam-spring model treats the lining as a series of discrete segments, connected through reactive springs that simulate ground-structure interaction.

Beam-spring models can be further classified based on how joint behavior is incorporated, as illustrated in Fig. 1: the rigid joint method, the rotational spring method, and the hinge method (Kim et al., 2006). The rigid joint method models the lining as a continuous member with constant flexural stiffness (EI), thereby failing to account for the reduced stiffness at joints and resulting in an overestimation of internal moments. The rotational spring method represents the interaction between the ground and the lining using axial and shear elastic links, with the ground modeled as linear springs under plane strain conditions. However, this approach also has limitations, including assumptions of linear elasticity and neglect of joint stiffness ratios and spatial distribution. The hinge

method simplifies the joints as mechanical hinges, which may realistically simulate behavior in stiff ground conditions but tends to predict excessive deformation in soft ground, resulting in a significant discrepancy from actual behavior.

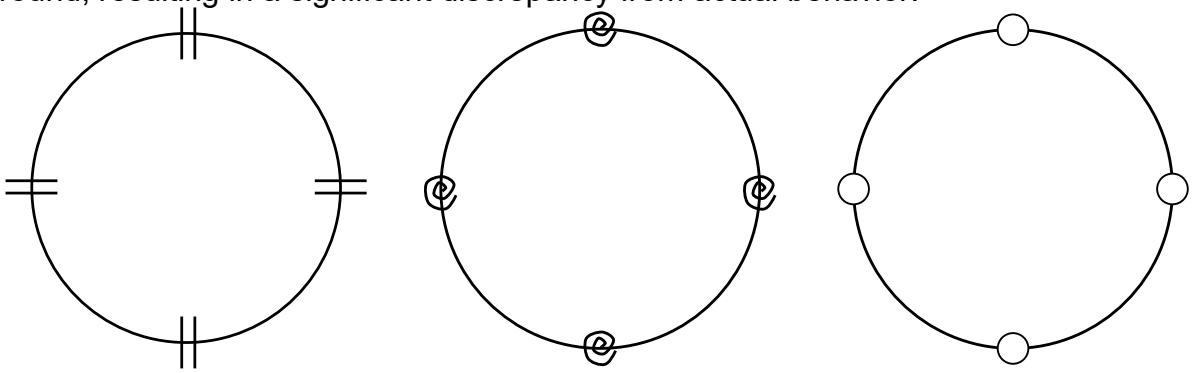

(a) Rigid (b) Rotary (c) Hinge

Fig. 1 Structural model of the segment lining

In this context, the two-ring beam-spring model (Fig. 2) has recently been adopted for more refined analysis. In this model, the radial joints are represented by rotational springs (K_m), the ring joints by shear springs (K_s), and ground reaction springs (K_r) are applied to the segments as shown in Eqs. (1)-(3). By incorporating the reduced stiffness at the joints, the model provides a more realistic stress distribution compared to the rigid joint model. Notably, in terms of the moment distribution relative to axial force, the rigid joint model estimates the maximum moment at the tunnel crown due to the assumption of uniform ring stiffness. However, in the two-ring model, the concentration of joints near the key segment results in relatively lower moments at the crown. This reflects the segmented nature of the segmental lining and is therefore considered to yield a more realistic representation of its structural behavior (Jee, 2020).

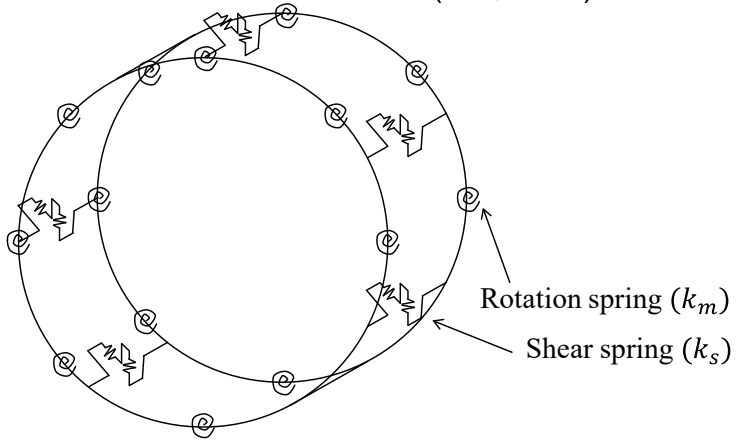

Fig. 2 Two-ring beam-spring model(Yamaguchi et al., 1978)

The segmental lining can be schematically illustrated as shown in Fig. 3, where M denotes the bending moment, θ the rotation angle, b the segment width, A_b the cross-sectional area of the bolt, and x the distance from the compressive edge to the neutral

axis. h represents the segment thickness, d the effective depth, and n the modular ratio of the elastic moduli of concrete and reinforcement. Based on these parameters, the rotational spring stiffness (K_m) and ground reaction spring stiffness (K_r) can be calculated, while the shear spring stiffness (K_s) is typically assumed to be 40 MN/m.

$$K_r = \frac{E}{R} \quad (1)$$

$$K_m = \frac{M}{\theta} = \frac{x(3h-2x)bE}{24} \quad (2)$$

$$x = \frac{nA_b}{b}\left(\sqrt{\frac{2bd}{nA_b}} - 1\right) \quad (3)$$

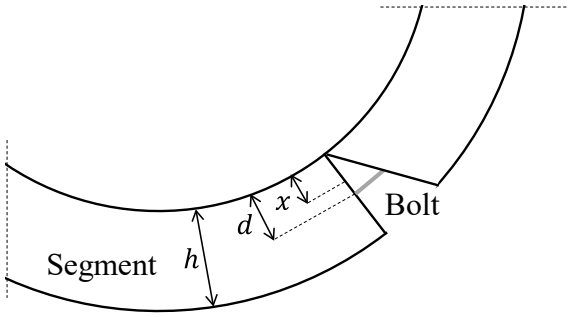

Fig. 3 Physical model for rotational spring calculation condition

However, the two-ring beam model also has limitations. For example, it is difficult to explicitly capture the relative displacements between segments or to quantitatively extract the deformation of individual segments. Furthermore, when performing three-dimensional analysis using the continuum-based Non-Joint Mode (NJM), the segmented behavior between rings cannot be adequately represented.

To overcome these limitations, this study introduces the Break-Joint Mode (BJM), which considers the interfaces between segments. The objective is to accurately reflect the discontinuous behavior of segmental linings under various loading conditions and to evaluate the validity and applicability of the BJM by comparing its results with those of the NJM and actual construction cases.

2.2 Break-joint mode analysis method

The Break-Joint Mode (BJM) is an analytical method developed to realistically simulate the discontinuous behavior of segmental tunnel linings. It accounts for the discontinuities and frictional interactions at the joints between segments, thereby enabling a more accurate representation of the actual structural response. In contrast, the conventional continuum-based Non-Joint Mode (NJM) does not consider the separation or frictional behavior at segment joints, resulting in an overly continuous stress distribution that may not reflect real-world conditions.

BJM incorporates interface elements at segment joints, characterized by specific friction coefficients and stiffness parameters, to represent physical behaviors such as separation, rotation, and sliding. This modeling approach captures the loss of structural

continuity and the localized interaction at joints, which are critical in the performance of shield TBM tunnels.

The method simulates the interaction between the ground and the segment lining using elastic springs and interface elements, effectively modeling the coupled behavior caused by frictional forces and stress discontinuities. As such, it is particularly suitable for shield TBM tunnels with highly segmented linings. In this study, a three-dimensional model implementing BJM is used to compare the stress distribution with NJM and analyze the influence of segmental effects on actual structural behavior.

2.3 Interface configuration between segments

The intersegmental interface model is based on Coulomb's friction theory (1785), as expressed in Eq. (4), and defines the frictional resistance in the normal and tangential directions according to the normal confinement force and the friction angle. This relationship is further refined by Yi and Song (2023a), as described in Eq. (5)-(6). The interface elements are primarily governed by two parameters: the normal stiffness coefficient (k_n) and the shear stiffness coefficient (k_t), by Brinkgreve et al., (2015) which are calculated using the elastic modulus of the adjacent material, an empirical stiffness reduction factor (R), and an assumed virtual thickness (t_v).

$$f = \sqrt{t_v^2} + t_n tan\phi(\kappa) - c(\kappa) = 0 \tag{4}$$

$$k_n = \frac{E_{oed,i}}{t_v}, k_t = \frac{G_i}{t_v} \tag{5}$$

$$E_{oed,i} = \frac{2G_i(1-\nu_i)}{1-2\nu_i}, \quad G_i = R^2 G_{soil}, \quad G_{soil} = \frac{E}{2(1+\nu_{soil})} \tag{6}$$

The parameters employed in the interface formulation are commonly used in finite element analysis to define the interaction between ground and structure. The stiffness reduction factor (R) is determined based on material type, as summarized in Table 1. The creep Poisson's ratio (ν_a) is typically assumed to be 0.18, while the interface Poisson's ratio (ν_i) is set to 0.45 to simulate incompressible frictional behavior and mitigate numerical instability. The virtual thickness of the interface (t_v) generally ranges from 0.01 to 0.1, with smaller values recommended when there is a significant stiffness contrast between adjoining materials.

Table 1. Range of related stiffness reduction factor in numerical analytical application of Coulomb friction function equations (Brinkgreve et al., (2015))

Sandy soil / Steel	Clay soil / Steel	Sandy soil / Concrete	Clay soil / Concrete
0.6 ~ 0.7	0.5	1.0 ~ 0.8	1.0 ~ 0.7

In the numerical model, interface elements are located at the segment joints. Upon generation, the elements automatically introduce node separation and create components with specific stiffness in the normal and tangential directions. This configuration enables precise simulation of contact, separation, sliding, and rotational

behavior between segments. Additionally, as shown in Fig. 4, the intersegmental interface elements possess three translational degrees of freedom and one rotational degree of freedom. The stiffness matrix of interface element is expressed as Eq. (7), incorporating rotational degrees of freedom. The stiffness is calculated using Eq. (8), which divides the elastic modulus of the surrounding material by a characteristic length. The characteristic length (l_{ch}) is taken as the thickness of the element (Yi and Song, 2023b).

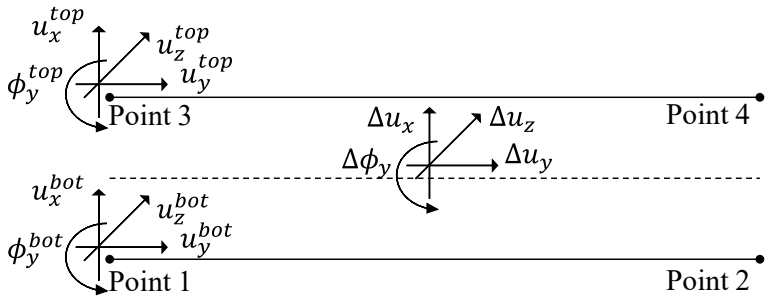

Fig. 4 Relative displacement and interfacial force of interface elements

$$D = \begin{bmatrix} k_n & 0 & 0 & 0 \\ 0 & k_t & 0 & 0 \\ 0 & 0 & k_t & 0 \\ 0 & 0 & 0 & \frac{k_t t^3}{12} \end{bmatrix} \quad (7)$$

$$k_n = \frac{\alpha E}{l_{ch}}, \quad k_t = \beta k_n \; or \frac{\beta G}{l_{ch}} \quad (8)$$

α and β are conversion factors, while E and G represent the elastic modulus and shear modulus, respectively. These conversion factors must be chosen empirically. If the values are too large, numerical instability may occur; if too small, the interface element may not accurately capture relative displacements. Typically, values ranging from 0.1 to 10 are used (MIDAS I.T., 2013; Park et al., 2019). When applied to the interfacial boundaries of segmental linings, this approach can reproduce discontinuous stress distributions that closely resemble actual behavior.

3. NUMERICAL MODELING AND ANALYSIS CONDITION

3.1 Modeling configuration for static and dynamic analysis

The numerical modeling based on the Break-Joint Mode (BJM) was developed to analyze the static and dynamic behavior of segmental tunnel linings. For the static analysis, the model was constructed based on a case study of a tunnel constructed in Korea. In the dynamic analysis, the same segmental lining geometry and material properties were adopted, and a single soil stratum composed of relatively low-stiffness

soft sedimentary ground was assumed. To minimize the effect of wave reflection caused by external dynamic loads, the bottom boundary of the model was extended to a depth equivalent to three times the tunnel diameter, and symmetric boundary conditions were applied in all directions to ensure the accuracy of the analysis. The configurations of the static models are shown in Fig. 5, and the cross-sectional geometry of the segmental lining is illustrated in Fig. 6. The structural material properties of the segment lining are summarized in Table 2.

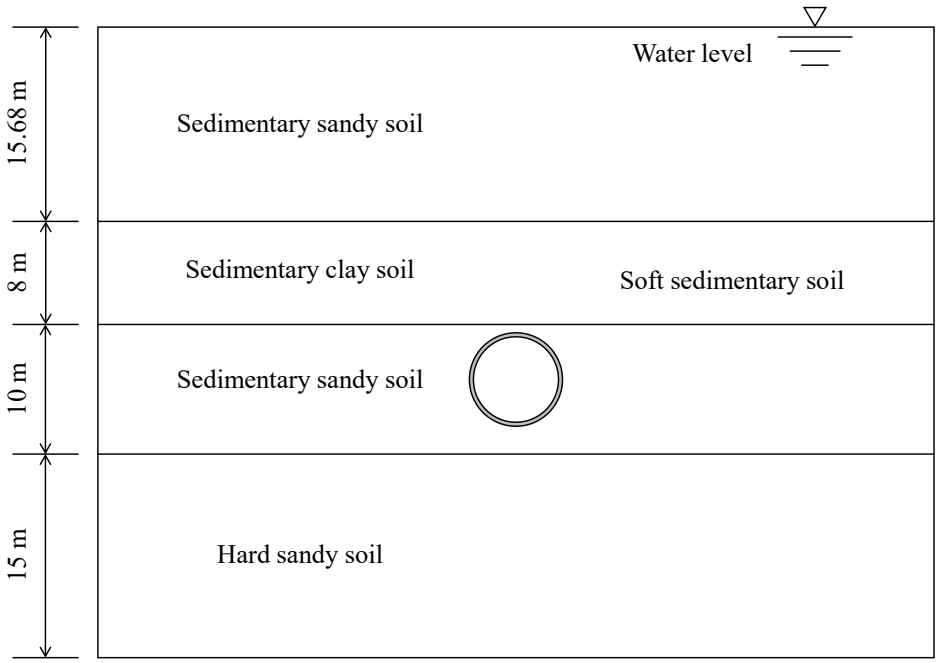

Fig. 5 Numerical model geometry for static and dynamic analysis of segmental linings

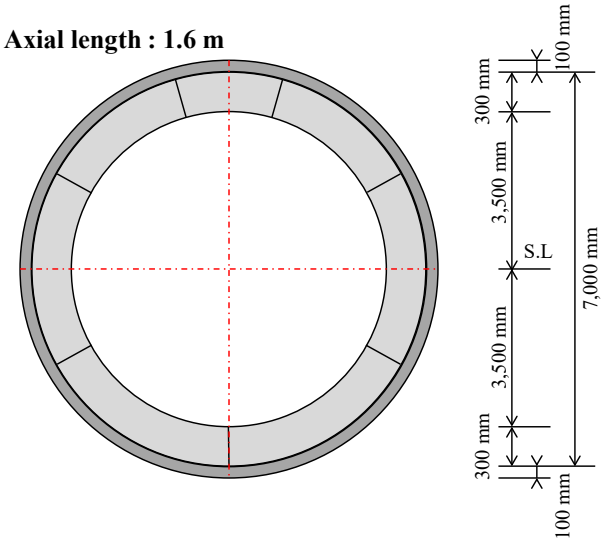

Fig. 6 Section configuration diagram of segmental lining

Table 2. Properties of structural materials used in modeling

Materials	Unit	Segment lining	Backfill grouting	Steel material
Model type	-	Isotropic Elastic	Isotropic Elastic	Isotropic Elastic
Materials model	-	2D Shell	3D Solid	3D Solid
Unit weight	kN/m^3	25	21	74
Elastic modulus	kN/m^2	2.5E+06	0.4E+07	2.1E+08
Friction angle	Deg	-	38	-
Cohesion	kN	-	100	-
Poisson's ratio	-	0.18	0.25	0.30

3.2 Components of interface modeling based on the Break-Joint Mode (BJM)

The normal stiffness coefficient (k_n) and shear stiffness coefficient (k_t) of the interface elements between segments are based on Coulomb's friction theory (1785) and are implemented in finite element analysis (FEM) to represent the interaction behavior between the ground and the structure. These stiffness parameters are initially calculated using Eq. (8), but direct application without calibration results in excessively large values, leading to analysis outcomes similar to those obtained from the Non-joint Mode (NJM), thereby failing to properly reflect segmentation effects.

Ideally, the calibration of stiffness coefficients should be based on experimental results considering the materials and acting forces at the interface between adjacent segments. However, in this study, sensitivity analysis was employed to determine the appropriate stiffness values. Specifically, the interface stiffness was adjusted to produce a clear stress discontinuity at the segment joints located at the center ring of the tunnel. The derived coefficients are relative rather than absolute, and while the location or extent of segmentation effects may vary with loading conditions, the reliability of the overall analysis remains unaffected.

The sensitivity analysis revealed that reducing the initially calculated stiffness values from Eq. (8) by successive factors of 10^{-n} enabled the segmentation effect to become evident, as stresses at the joints approached zero. Accordingly, this study adopted a final stiffness coefficient equal to the value obtained from Eq. (8) multiplied by 10^{-6}.

The final values of the normal and shear stiffness coefficients applied to the segment interfaces are summarized in Table 3, and their application within the segment model is illustrated in Fig. 7. The results confirm that the interface-induced discontinuity due to the absence of shared nodes between segments dominates the structural response. Therefore, the realistic modeling of segmentation behavior is more influenced by interface separation than by the absolute magnitude of k_n and k_t.

Table 3. Properties of of interface element material for Break-joint mode

Properties	Model Type	Vertical stiffness Coefficient (k_n) (kN/m^3)	Shear stiffness coefficient (k_t) (kN/m^3)	Friction angle (deg)	Cohesion (kN/m^2)
Interface	Plane & Shell	1.20E+05	2.43E+03	10	5

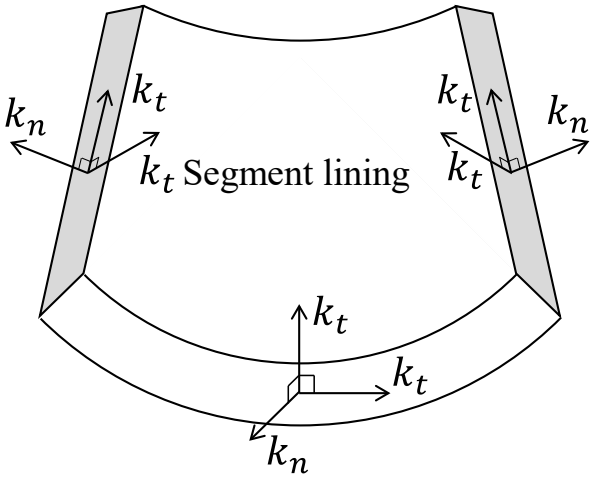

Fig. 7 Interface-integrated numerical model of segmental lining

3.3 Definition of loading conditions in the BJM model

In the static analysis, two primary loading conditions were considered. A representative section with a diameter of 7.0 m, corresponding to a shield TBM tunnel typically used for railways, was selected. The geometric configuration of this section is illustrated in Fig. 6, and the structural and material properties of the segment lining were determined based on domestic construction case studies. The analysis domain and ground conditions, as depicted in Fig. 5, reflect a multilayered soil profile incorporating both actual subsurface conditions and groundwater level variations. Geotechnical properties are summarized in Table. 4.

The first loading condition evaluates the stress and deformation behavior of the segment lining under the self-weight of the overburden. The analysis stages for this condition are summarized in Table 5. The second condition focuses on the response of the segment lining to groundwater level fluctuations. This scenario was analyzed using a stress–seepage coupled analysis approach, with the corresponding analysis stages presented in Table 6.

Table 4. Properties of ground materials applied to modelling

Materials	Unit	Sedimentary sandy soil	Sedimentary clay soill	Sedimentary sandy soil	Hard sandy soil
Unit weight	kN/m^3	17	18	18	18
Elastic modulus	kN/m^2	7,000	4,000	10,000	25,000
Friction angle	Deg	20	0	22	27
Cohesion	kN	0	20	5	0
Poisson's ratio	-	0.37	0.4	0.36	0.36
Initial void ratio	-	0.5	1.29	0.5	0.5
Permeability	cm/s	9.3 × 10-4	4.1 × 10-7	5.9 × 10-4	4.6 × 10-4

Table 5. Construction stage analysis sequence for analyzing stress and deformation results due to earth pressure

Stage	Detail		Note
	Non joint mode	Break joint mode	
1	In-situ	In-situ, Activate of the segment rigid links	
2	Excavation and lining installation (+ backfill grouting)	Excavation and lining installation, activate of the segment interface element(+ backfill grouting)	
3		Non-activate of the segment rigid links	Segment to segment node separation

Table 6. Analysis modeling steps for analyzing groundwater level change

Stage	Detail		Analysis type
	Non joint mode	Break joint mode	
1	-In-situ -Apply of water level boundary conditions	-In-situ -Apply of water level boundary conditions -Activate of segment rigid links	Steady flow analysis B.C-1: Total Head = 23.7m
2	-Apply of gravitational weight -Apply of boundary condition	-Apply of gravitational weight -Apply of boundary condition	Stress analysis
3	-Excavation and lining installation -Backfill grouting installation	-Excavation and lining installation -Backfill grouting installation -Activate of the segment interface element	Stress analysis
4		-Non-activate of segment rigid links	Stress analysis
5 - 7	-Decrease in groundwater level	-Decrease in groundwater level	Unsteady flow analysis B.C-3: Joint Head = 11.5m
8 - 11	-Rise in groundwater levels	-Rise in groundwater levels	Unsteady flow analysis B.C-2: Joint Head = 23.7m

4. RESPONSE ANALYSIS ON STATIC LOADING

4.1 Comparison of segment lining response characteristics between NJM and BJM under earth pressure loading

The deformation behavior of segmental tunnel linings under static loading conditions was analyzed and compared with the results obtained from the conventional Non-Joint Mode (NJM) analysis to investigate its correlation with the actual damage mechanisms observed in segment linings. The length of the numerical model in the Y-direction (along the tunnel axis) was set to 4.8 meters, corresponding to the length of three segment rings. A nonlinear construction stage analysis was performed to simulate the deformation and stress of the tunnel cross-section, which was excavated through the ground under the influence of in-situ earth pressure. The detailed construction stages adopted in the analysis are summarized in Table 5.

In the BJM analysis, the segments were initially integrated using rigid link elements prior to the application of interface elements. Upon completion of the lining construction, the rigid links were removed to release the nodes between segments, and only the interface elements incorporating frictional behavior were applied to simulate the relative movements between segments. The analysis results revealed that BJM generally produced lower stresses in most sections of the lining compared to NJM. However, localized maximum stresses were found to be higher within certain regions of the overall model domain. Additionally, displacement discontinuities were observed at the locations where the rigid links were released.

These findings demonstrate that the resulting differential displacements between segments can potentially induce damage mechanisms observed in actual segmental linings, such as gasket failure, inner surface cracking, and outer surface openings, which in turn can lead to cracking, spalling, and leakage. Earth pressure is typically the dominant load acting on tunnel linings, and thus the associated internal forces and deformation behaviors were analyzed. Fig. 8 and Fig. 9 present the analysis results of the maximum bending moments and shear forces under these conditions.

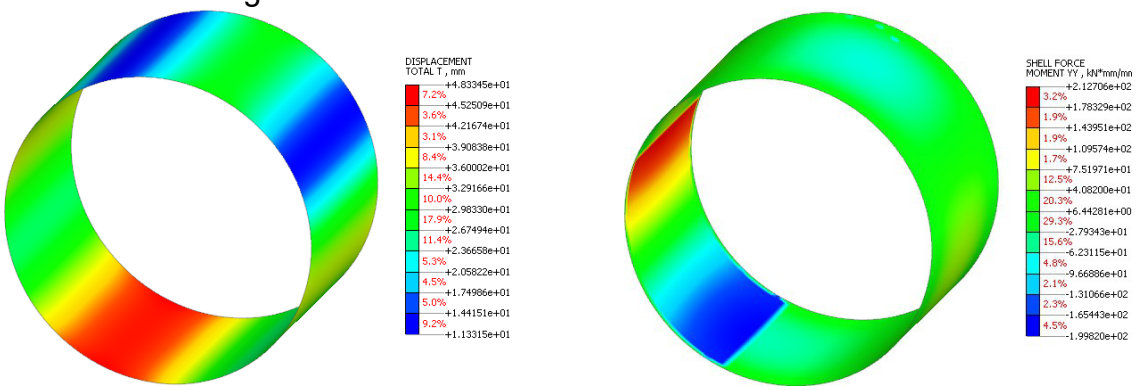

(a) Non-joint mode (b) Break-joint mode

Fig. 8 Comparison of vertical displacement of BJM and BJM after tunneling

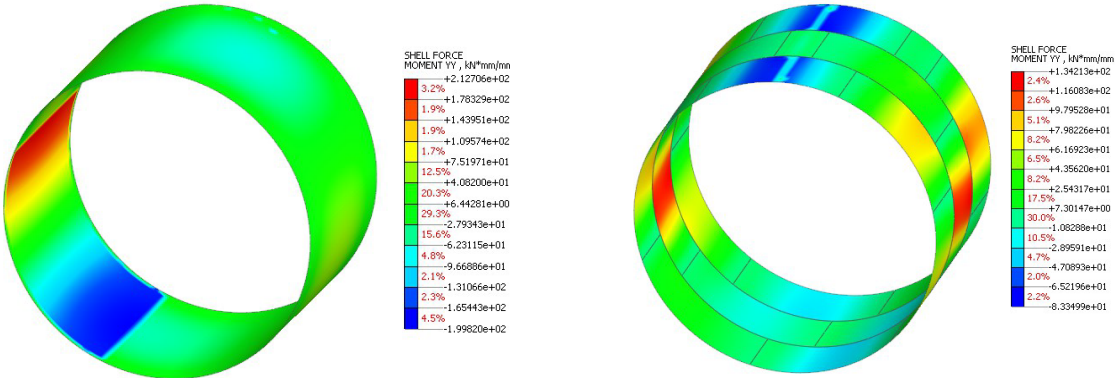

(a) Non-joint mode (b) Break-joint mode

Fig. 9 Comparison of Bending moment of BJM and BJM after tunneling

4.2 Differences in Deformation Behavior Between NJM and BJM Under Groundwater Level Fluctuations

The most significant difference in deformation behavior between the Non-Joint Mode (NJM) and Break-Joint Mode (BJM) under identical loading conditions was observed under conditions of significant groundwater table fluctuations. The analysis of groundwater level lowering, rising, and recovery was performed using stress–seepage coupled analysis, with the analysis stages summarized in Table 6. The seepage analysis results for Stages 1 and 5–7 are presented in Fig. 10. The comparative results of the deformed shapes are shown in Fig. 11, where both the pre- and post-deformation shapes of the lining are displayed simultaneously. The unshaded circular line represents the initial lining geometry before deformation, and the deformation diagrams are scaled for clarity rather than presenting actual displacement magnitudes. Under groundwater level drawdown, the NJM results show an overall downward settlement of the entire lining, whereas the BJM results show downward displacement at the crown and upward displacement at the invert.

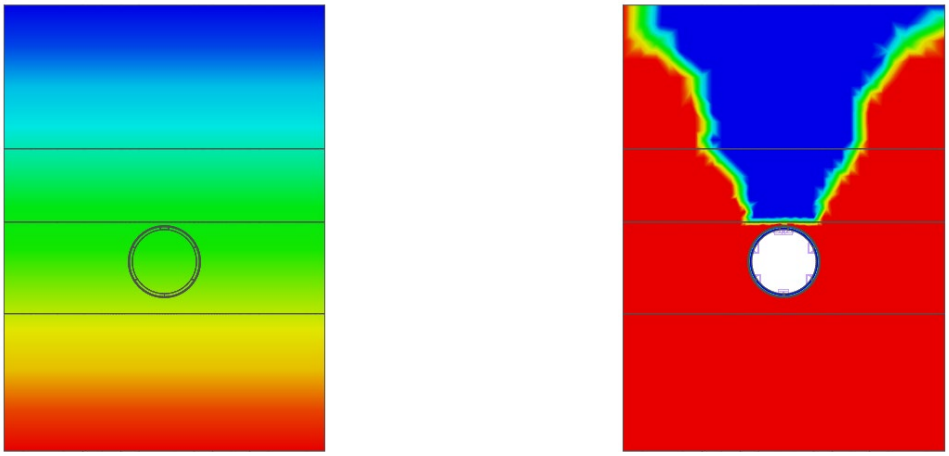

(a) Steady flow analysis (b) Stage 5-7. Unsteady flow analysis

Fig. 10 Seepage analysis result diagram

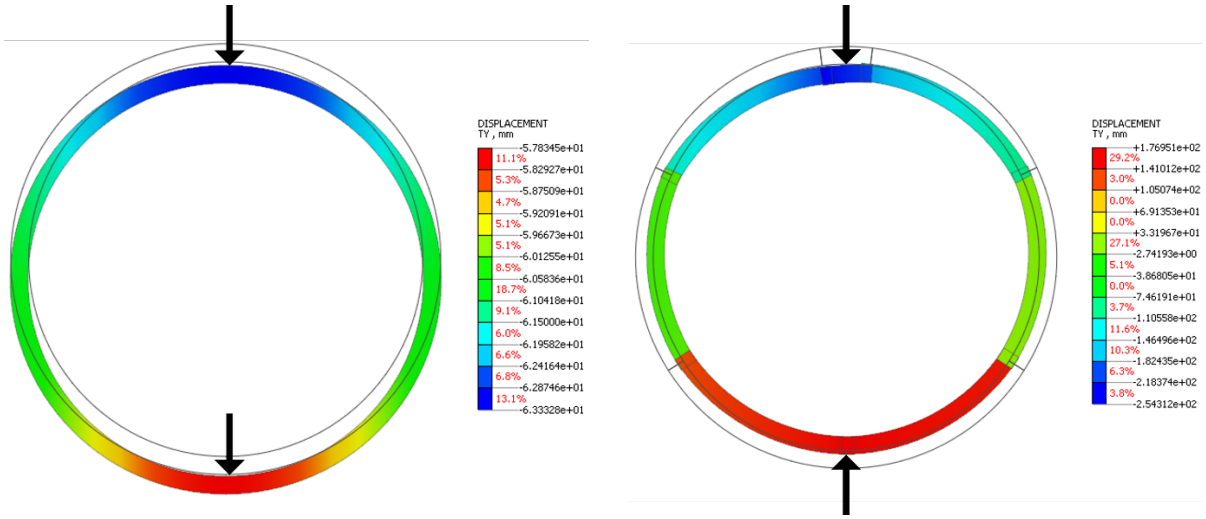

(a) Deformation of lining (NJM) (b) Deformation of lining (BJM)

Fig. 11 Comparison of NJM and BJM on lining deformation due to groundwater level drops

Ovality(O_R), defined as the ratio of the major to minor diameters of the tunnel lining(Eq. (9)), is a commonly used indicator for assessing segmental lining deformation, although no universal quality standard exists (Yang et al., 2018; Kolic and Mayerhofer, 2011). In the BJM results, the ovality of the tunnel lining increased significantly under groundwater drawdown conditions. As shown in Fig. 12, the NJM model produced an ovality of 1.3 ‰ with a major diameter of 7.003 m and a minor diameter of 6.994 m (Fig. 12(a)), whereas the BJM model yielded an ovality of 107.6 ‰ with a major diameter of 7.276 m and a minor diameter of 6.569 m (Fig. 12(b)), resulting in an ovality difference of 106.3 ‰ between the two methods.

$$O_R = \frac{D_{max} - D_{min}}{D_{min}} \quad (9)$$

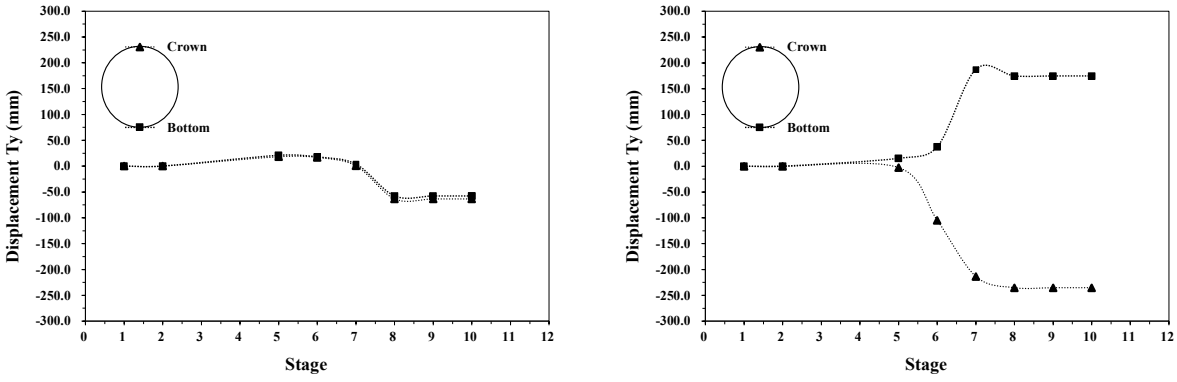

(a) NJM displacement result of water level changes (b) BJM displacement result of water level changes

Fig. 12 Comparison of ovalization of NJM and BJM due to groundwater level changes

This pronounced difference reflects the combined effects of increased upper earth pressure due to changes in the unit weight of the overburden and the uplift force acting at the tunnel invert. The NJM, based on the rigid-body assumption, fails to accurately reproduce actual deformation behavior, and thus the resulting stress distribution may deviate substantially from real-world conditions.

Fig. 13 presents empirical data from an actual shield TBM tunneling project conducted in soft ground conditions at the site. The figure illustrates the effects of shield TBM tunneling on longitudinal alignment accuracy, initial ovality, and significant ovality increases following groundwater level reductions. In the section around the 8,500-meter mark, initial ovality of approximately 40‰ was observed during the early construction phase. Subsequently, this section experienced longitudinal and transverse displacements along with cross-sectional deformation due to two incidents of groundwater drawdown. Although this section initially exhibited ovality similar to the adjacent areas, the ovality increased by up to an additional 45‰ following the groundwater lowering events. These field observations provide empirical validation of the ovality amplification behavior under groundwater level fluctuations, as previously demonstrated in the BJM analysis results shown in Fig. 12.

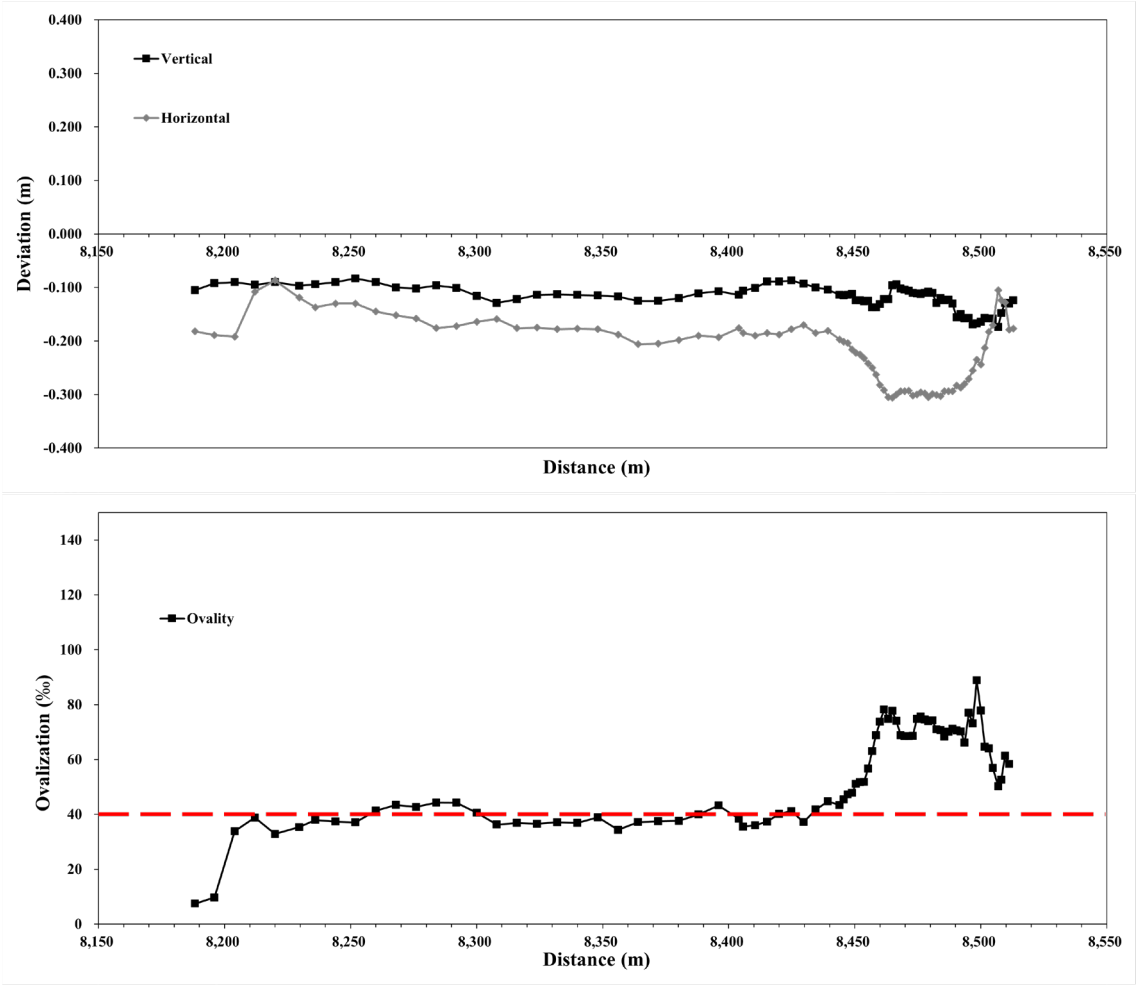

Fig. 13. Case on the straightness and ovality of shield TBM tunnel in soft ground

In the case of Earth Pressure Balance (EPB) shield TBM tunnels with large excavation diameters of approximately 7 meters, the total weight of the shield TBM machine can reach around 4,500 kN. The excavation stability of shield TBM machines depends not only on ground strength but also on various factors such as groundwater level, permeability, and deformability. According to the International Tunnelling and Underground Space Association (ITA) checklist for ground conditions and shield TBM applicability (Kim et al., 2021), the recommended standard penetration test (SPT) N-values are at least 10 for sandy soils and between 5 and 10 for alluvial sandy clay layers. However, in cases where the planned tunnel alignment passes beneath rivers or through zones of soft ground, segmental linings are often constructed in soils with lower strength than the recommended values.

Under such conditions, shield TBM machines frequently deviate from the designed alignment and require repeated correction processes to return to their intended path. During these adjustments, involving head-up and head-down movements of the shield machine, significant damage can occur to the previously installed segmental linings due to the application of unbalanced thrust forces. This process leads to increased segment offsets, which serve as major pathways for water leakage, and it also exacerbates ovality deformation of the segmental lining due to unbalanced earth pressures.

Among the various factors contributing to the increase in ovality—representative of deformation in shield TBM segmental linings—earth pressure is the most significant. Large deformations can still occur after construction if asymmetric earth pressures persist. Additional ovality increases are often observed under asymmetric earth pressures induced by surface surcharge loads (Kolic and Mayerhofer, 2011).

5. CONCULUSIONS

This study presented a novel numerical modeling approach, the Break-Joint Mode (BJM), which explicitly considers the discontinuous nature of shield TBM segmental linings. Unlike conventional analysis methods, such as the Non-Joint Mode (NJM) and the two-ring beam-spring model, the BJM fully separates the segments and excludes the structural effects of bolts and shear keys. Instead, it introduces frictional interface elements with only normal and shear stiffnesses to realistically simulate the contact behavior between segments and rings.

Through extensive numerical analyses under various static and dynamic loading conditions, it was confirmed that while both BJM and NJM produced similar global deformation patterns and stress distributions, the BJM exhibited significant differences at the segment level. Specifically, the BJM effectively captured independent stress distributions and localized stress concentrations at segment corners, caused by relative displacements between segments. These findings demonstrate that BJM can realistically simulate actual damage mechanisms frequently observed in shield TBM tunnels, such as joint offsets, cracking, breakage, spalling, and leakage—features that are difficult to capture with conventional modeling approaches.

Furthermore, this study critically reviewed the existing ovality criteria for segmental linings, which are typically set at 5‰ to 10‰ in many countries. It was found that such criteria lack structural justification, largely because conventional analysis methods are unable to predict the actual ovality limits corresponding to safe structural performance. In this study, ovality values exceeding 10‰ were readily observed under self-weight

alone, with values up to 30‰ occurring under additional construction-induced deformations. Even under dynamic loads such as seismic events, the impact of ovality on structural stability was minimal, given the inherently high material strength of segmental linings. Based on the BJM results, it is suggested that ovality values up to 50‰ may still ensure sufficient safety margins, although this tentative conclusion requires further verification through comprehensive studies considering various tunnel diameters, segment strengths, and loading conditions.

The significance of this study lies in providing an alternative modeling approach that explicitly reflects the discontinuous characteristics of shield TBM segmental linings, offering deeper insight into their actual structural behavior and damage mechanisms. While the two-ring beam-spring model remains widely used for cross-sectional design, and three-dimensional analyses typically rely on continuum models that ignore segmentation, this study demonstrates the potential of BJM in more realistically simulating three-dimensional structural performance by explicitly considering segmental discontinuity.

Nevertheless, it should be noted that the determination of interface stiffness coefficients (normal and shear) in this study was conducted empirically through trial-and-error methods based on observed stress discontinuities. Although this approach effectively captured the segmentation effects in the present study, it may not yet be generalized for broader applications. Therefore, future research should focus on establishing a more systematic and generalized calibration method for interface stiffness parameters, incorporating extensive parametric analyses under diverse conditions.

In conclusion, the Break-Joint Mode provides a more structurally realistic and mechanically rational framework for the analysis and design of shield TBM segmental linings. It offers enhanced predictive capability for localized deformation behaviors and damage risks, potentially contributing to improved design practices and performance-based standards for segmental tunnel linings.

REFERENCES

Brinkgreve, R.B.J., Kumarswamy, S., and Swolfs, W.M. (2015), *Reference Manual, Plaxis 3D 2015 User's Manual*, Plaxis bv, Delft, Netherlands, pp. 1-284.

Gharehdash, S., and Barzegar, M. (2015), "Numerical modeling of the dynamic behaviour of tunnel lining in shield tunneling," *KSCE Journal of Civil Engineering*, **19**(6), 1626-1636.

Jee, W. (2020), *Modern Tunnel Design Technology*, CIR Publishing, Seoul, pp. 205-209.

Kim, G.S., Kim, H.J., Lee, H.W., and Jung, D.H. (2006), "Joint characteristics of shield tunnel segment lining using structural analysis models," *Proceedings of the KSCE 2006 Convention*, Gwangju, Korea, pp. 4696-4699.

Kim, N.Y., Kang, H.T., Lee, K.H., Lee, S.R., (2021), "Development of TBM design criteria and specification for large section road tunnel", Traffic Research Institute of the Korea Expressway Corporation, pp. 125.

Kolic, D., and Mayerhofer, A. (2011), "Segmental lining tolerances and imperfections," *Proceedings of the ITA WTC 2009 Symposium*, Budapest, Hungary, pp. 8-15.

Korea Construction Standards Center (2019), *KC CODE KDS 64 17 00*, Ministry of Land, Infrastructure and Transport, Seoul, Korea, pp. 24-25.

Lydon, F.D., and Balendran, R.V. (1986), "Some observations on elastic properties of plain concrete," *Cement and Concrete Research*, **16**(3), 314-324.

Ministry of Land, Transport and Maritime Affairs (2011), *Road Design Manual, Part 6: Tunnels*, Seoul, Korea, pp. 616-648.

Park, M.C., Kwon, O.K., Kim, C.M., Yun, D.K., and Choi, Y.K. (2019), "Study (V) on development of charts and equations predicting allowable compressive bearing capacity for prebored PHC piles socketed into weathered rock through sandy soil layers – Analysis of results and data by parametric numerical analysis –," *Journal of the Korean Geotechnical Society*, **35**(10), 47-66.

Yang, Y., Zhou, B., Xie, X., and Liu, C. (2018), "Characteristics and causes of cracking and damage of shield tunnel segmented lining in construction stage – a case study in Shanghai soft soil," *European Journal of Environmental and Civil Engineering*, **22**(Sup 1), s213-s227.

Yamaguchi, Y., Kawada, H., and Yamazaki, M. (1978), "Comparison between design models applied to segmental tunnel linings," *Structure Design Documents by Japan Railway Civil Engineering Association*, 3-8.

Yi, G.J., and Song, K.I. (2023a), "Dynamic response of segment lining due to train-induced vibration," *Journal of Korean Tunnelling and Underground Space Association*, **25**(4), 305-330.

Yi, G.J., and Song, K.I. (2023b), "The effect of tunnel ovality on the dynamic behavior of segment lining," *Journal of Korean Tunnelling and Underground Space Association*, **25**(6), 423-446. doi:10.9711/KTAJ.2023.25.6.423.